I&EC research
Industrial & Engineering Chemistry Research

Article

Cite This: Ind. Eng. Chem. Res. 2019, 58, 7063−7073

pubs.acs.org/IECR

Toward Sustainable and Complete Wood Valorization by Fractionating Lignin with Low Condensation Using an Acid Hydrotrope at Low Temperatures (≤80 °C)

Jinlan Cheng,[†,‡] Kolby Hirth,[†] Qianli Ma,[†,§] Junjun Zhu,[†,‡] Zhaojiang Wang,[†,∥] and J. Y. Zhu*[,†]

[†]USDA Forest Service, Forest Products Laboratory, Madison, Wisconsin 53726, United States

[‡]Jiangsu Co-innovation Center for Efficient Processing and Utilization of Forest Resources, Jiangsu Provincial Key Lab Pulp & Paper Science and Technology, Nanjing Forestry University, Nanjing 210037, China

[§]State Key Lab Pulp and Paper Eng., South China University of Technology, Guangzhou 510640, China

[∥]State Key Laboratory of Biobased Material and Green Papermaking, Qilu University of Technology, Shandong Academy of Sciences, Jinan 250353, China

ABSTRACT: Poplar wood was fractionated under a range of conditions using an inexpensive and recyclable commercial aromatic acid, *p*-toluenesulfonic acid (*p*-TsOH), as an acid hydrotrope (AH). The fractionated cellulose-rich solid fraction demonstrated excellent physical and optical properties as papermaking fibers. The dissolved xylose can be dehydrated into furfural using the *p*-TsOH in the spent liquor without additional catalysts. The acid hydrotrope dissolved lignin (AHL) has high *β*-aryl ether linkage content (~60%) and high molecular weight (~4000 Da), similar to that of mill wood lignin (MWL). Increasing acid hydrotrope fractionation (AHF) severity increased AHL yield, but reduced *β*-aryl ether bonds, decreased molecular weight and increased AHL glass transition temperature. An AHL yield of 50% can be obtained while retaining approximately half of the *β*-O-4 linkages, beneficial for lignin valorization as a polymer in composites as well as for production of monomers or aromatics through subsequent depolymerization.

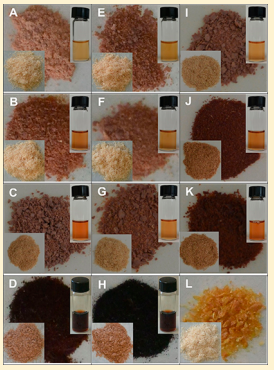

INTRODUCTION

Energy crops such as poplar wood can grow on marginal land has attracted great interest in the agriculture community.[1] Poplar has many advantages as energy feedstock for its well-known silviculture and ease of propagation.[2] Economic and efficient utilization of energy crops such as poplar wood through the biorefinery concept can not only replace many petroleum-based chemicals, fuels, and products but also promote opportunities in rural America for sustainable economic development. Toward this goal, many fractionation processes have been developed[3−7] along with industrial wood pulping processes to valorize carbohydrates in lignocellulosic biomass for producing sugars, biofuels, or papermaking and textile fibers. These processes are operated at high temperatures and use harsh chemicals with a primary focus on efficient separation or bioconversion of carbohydrates. The resultant lignin, the second major component of lignocelluloses, is chemically modified, highly condensed, and therefore difficult valorize.[8−11] Current commercial alkaline wood pulping operations burn lignin for pulping chemical recovery and energy; however, lignin valorization for producing chemicals and bioproducts is a necessity for, and remains a central challenge to, economic and sustainable development of future biorefineries.[12−14] Addressing this central challenge requires new fractionation strategies that prioritize both carbohydrate and lignin valorization.

The substantial reduction of ether bond linkages, mainly *β*-O-4, in most fractionation and commercial wood pulping processes, has been recognized as the major cause of difficulties in downstream lignin depolymerization into aromatics for valorization.[9,15,16] Slow and mild acidolysis or organic solvent extraction can avoid lignin condensation but has very low lignin yield even at prolonged reaction time and is therefore not suitable for commercial practice. Elegant stabilization chemistry has been developed to protect lignin from condensation but has issues related to chemical toxicity.[8] A "lignin-first" biorefinery concept using a one-step reductive catalytic lignin fractionation (RCF) (i.e., directly catalyze raw biomass with native state lignin into lignin aromatics) has been proposed to avoid lignin condensation.[15−18] Effective implementation of the concept, however, requires efficiently valorizing the carbohydrate fraction and recovering the catalyst,[16,19] which often involves a second step, as recently demonstrated.[18] In this sense the conventional two-step valorization approach (i.e., first step fractionation to produce uncondensed lignin and separate unmodified cellulosic fraction followed by subsequent processing or depolymerization of lignin) can be a potentially more desirable pathway, because

Received: February 17, 2019
Revised: April 4, 2019
Accepted: April 8, 2019
Published: April 18, 2019

DOI: 10.1021/acs.iecr.9b00931
Ind. Eng. Chem. Res. 2019, 58, 7063−7073

high yield of lignin monomer or aromatics can be obtained from uncondensed lignin using a variety of available catalytic processes[14,20] including those used in the lignin-first biorefinery concept.[15−17] A few elegant studies have demonstrated this possibility using lignin with minimal condensation.[21−24] Furthermore, lignin with low condensation can be directly valorized as high-molecular-weight polymers, such as in composites, without further depolymerization.[25,26] The key objective is to develop simple, sustainable, efficient, and low-cost fractionation processes that can sufficiently preserve the chemical structures of both lignin and cellulose.

Here we demonstrate an acid hydrotropic fractionation (AHF) process using *p*-toluenesulfonic acid (*p*-TsOH) to fractionate poplar wood lignin with low degrees of condensation at low temperatures (i.e., below the water boiling point) while preserving cellulose structure as fiberous materials. The acid hydrotrope solubilizes wood lignin, primarily through physical aggregation.[27−29] The dissolved acid hydrotropic lignin (AHL) can be precipitated by dilution with water to the minimal hydrotrope concentration (MHC),[29] similar to salt-based hydrotropic fractionation. It differentiates from salt-based hydrotropic fraction that is carried out at a high temperature of 150 °C or high for 4−6 h for wood pulping[30] or for enzymatic sugar production.[31,32] Low-temperature AHF allows for production of lignin with low degrees of condensation. With acid *p*-TsOH, the dissolved xylan by AH can be dehydrated into furfural catalyzed by the acid in the spent liquor without additional catalysts. The acid hydrotrope, *p*-TsOH, can then be reused or recycled after lignin precipitation, reconcentration, and distillation of furfural, the study of which is the object of ongoing research.

The present study differentiates from our earlier study[29,33] by focusing on (1) evaluating the properties of AHF cellulosic fibers and (2) two-dimensional ^{13}C-^{1}H nuclear magnetic resonance (NMR) analyses of AHL and validating the hypothesis proposed:[29] Low-temperature acid hydrotrope fractionation (AHF) can produce lignin with low degrees of condensation together with cellulose with insignificant degradation. With the features of low temperature, and therefore low pressure, and the potential ease of acid recovery, AHF opens a promising avenue for achieving low cost and sustainable fractionation and complete valorization of lignocelluloses.

MATERIALS AND METHODS

Materials. Poplar NE222 logs (*Populus deltoides* Bartr. ex Marsh. × *P. nigra* L.) were from the Hugo Sauer Nursery in Rhinelander, WI, provided by Dr. Ronald Zalesny, Jr., of USDA Forest Service, Northern Research Station. The age of the trees at harvest was 14 years. The logs were manually debarked and chipped at the USDA Forest Products Laboratory, Madison, WI. The chips were hammer-milled into 20 mesh fiber bundles. *p*-TsOH (ACS reagent-grade) was purchased from Sigma-Aldrich.

Preparation of Milled Wood Lignin (MWL). Air-dried wood chips were milled to pass 40 mesh in a Wiley mill (Model No. 2, Arthur H. Thomas Co.). Approximately 50 g of the mill wood powers were extracted using an aqueous acetone solution of volumetric concentration 90% for 8 h and turned 15 times in a Soxhlet extractor. The extracted wood was first air-dried in a large Petri dish followed by drying in a vacuum desiccator filled with phosphorus pentoxide. The dry, extracted wood powder was then milled in a vibratory ball mill. The ball-milled wood was dispersed in an aqueous dioxane solution with volumetric concentration of 96% followed by mechanical stirring. The wood loading was 4 g in 100 mL solution. After 24 h, the suspension was filtered using a sand core funnel filter. The solids were redispersed in fresh aqueous dioxane solution for additional 24 h. The liquid extracts were combined and then dried in a rotary vacuum evaporator to obtain MWL.

***p*-TsOH Fractionation of Poplar Wood.** Aqueous *p*-TsOH solutions at various concentrations of 25−67 wt % were prepared by solubilizing desired amounts of *p*-TsOH in deionized (DI) water. For each fractionation, acid solution to wood ratio 10:1 was used (i.e., 45 g of oven-dry (OD) poplar wood was fractionated in 450 g of the *p*-TsOH solution). Fractionation runs at ≤80 °C were conducted in a 1000 mL flask with *p*-TsOH heated to the desired fractionation temperature on a temperature-controlled shaking bed (Thermo Fisher Scientific, Model 4450, Waltham, MA) at 300 rpm, followed by the addition of poplar wood powder. Fractionation runs at 95 °C were conducted in a three-necked round-bottomed flask heated by a hot liquid glycerol bath on a heating plate. At the end of the preset fractionation time, 300 mL of DI water was added to dilute the acid concentration to terminate the reaction. Undissolved solids were separated from the corresponding spent liquor through vacuum filtration using filter paper (No. 2 Qualitative, Whatman). An aliquot of each spent liquor was collected for chemical composition analysis and the remainder was diluted to 2% acid concentration using water to precipitate AHL. After settling for 72 h, the diluted spent liquors were centrifuged at 10 000 rpm for 20 min. The supernatant was decanted and the precipitate collected. To remove the remaining *p*-TsOH, the collected AHL was dialyzed using DI water until conductance reached 1 $\mu\Omega^{-1}$ as measured by a conductance meter (YSI model 35, Yellow Springs Instrument, OH). The AHL was then freeze-dried for later use.

Chemical Composition Analyses. The undissolved solids, separated from filtration after each fractionation run, were thoroughly washed with DI water until neutral pH. Yields of washed water-insoluble solids (WIS) were determined gravimetrically based on the moisture contents and wet weights of the WISs. An aliquot of WIS sample was oven-dried at 105 °C and then Wiley-milled to 30 mesh powder after cooling. The Wiley-milled WIS and untreated poplar wood samples were hydrolyzed using two-step acid hydrolysis for chemical composition analyses using ion chromatography as described previously.[34] The spent liquors were analyzed for *p*-TsOH, acetic acid, and xylose using an HPLC system (Ultimate 3000, Thermo Scientific) equipped with a BioRad Aminex HPX- 87H column and a refraction index detector as described previously.[33]

Kinetics-Based Reaction Severity Analysis. Previously, we developed a combined hydrolysis factor (CHF)[35] and a combined delignification factor (CDF) that can effectively predict xylan dissolution and lignin solubilization by *p*-TsOH hydrotropic fractionation of wheat straw.[33] By using a biphasic reaction model[36,37] for both xylan and lignin (i.e., both xylan and lignin contains a fast and a slow fraction), the same expressions of CHF and CDF can be used in this study to predict poplar xylan and lignin dissolution through AHF using *p*-TsOH:

$$X_R = (1 - \theta)\, e^{-CHF} + \theta\, e^{-f\cdot CHF} \quad (1a)$$

DOI: 10.1021/acs.iecr.9b00931
Ind. Eng. Chem. Res. 2019, 58, 7063−7073

Table 1. Chemical Compositions of Water Insoluble Solids (WISs) and Spent Liquors from *p*-TsOH Batch Fractionated Poplar NE222 under a Range of Conditions[a]

			water insoluble solids (WIS)			spent liquor		
sample[b]	CDF; CHF	WIS yield (%)	glucan (%)	xylan (%)	kraft lignin (%)	xylose (g/L)	formic acid (g/L)	acetic acid (g/L)
NE222		100	45.7 ± 0.8	14.9 ± 0.5	23.4 ± 0.3			
P40T50t30	0.03; 0.01	97	43.4 (92)	16.0 (104)	22.5 (93)	0.08	0.08	1.2
P25T70t30	0.04; 0.04	96	45.0 (95)	16.4 (106)	23.3 (96)	0.1	0.2	1.7
P40T60t30	0.09; 0.03	96	43.9 (92)	16.2 (105)	22.5 (92)	0.1	0.2	1.8
P25T70t60	0.09; 0.06	94	45.4 (94)	15.9 (100)	22.7 (91)	0.4	0.1	3.1
P32T70t30	0.10; 0.06	92	46.0 (93)	15.6 (96)	22.6 (89)	0.2	0.2	2.2
P40T70t30	0.24; 0.15	95	45.2 (94)	15.9 (101)	23.1 (93)	0.2	0.2	2.2
P30T80t60	0.42; 0.46	84	50.7 (93)	13.4 (76)	23.1 (83)	1.4	0.3	3.3
P40T80t30	0.63; 0.65	78	53.0 (90)	10.6 (56)	20.1 (75)	0.4	0.2	2.5
P50T70t30	0.71; 0.40	84	52.1 (96)	12.9 (73)	20.5 (74)	0.5	0.3	2.8
P30T80t115	0.81; 0.89	78	54.5 (92)	9.0 (46)	23.4 (77)	7.5	0.5	4.3
P30T95t30	0.82; 1.9	72	55.6 (85)	7.1 (33)	22.3 (67)	10.2	0.7	4.3
P55T70t30	1.2; 0.66	77	55.9 (95)	10.9 (56)	19.2 (63)	1.8	0.5	3.4
P67T70t30	4.5; 2.2	65	64.8 (92)	7.5 (33)	15.9 (44)	8.8	0.4	3.8
P40T95t180	14.8; 31.5	62	71.4 (97)	4.1 (17)	12.9 (34)	16.6	0.6	4.3

[a]The numbers in the parentheses are the amount retained in WIS based on the corresponding component in the unfractionated poplar wood. [b]P*xx*T*yy*t*zz*: stands for *p*-TsOH concentration (wt %), temperature (°C), and fractionation time (min).

$$\mathrm{CHF} = \left[\exp\left(\alpha - \frac{E}{RT} + \beta C\right)\right]\cdot C\cdot t \tag{1b}$$

$$L_R = (1-\theta')\,e^{-\mathrm{CDF}} + \theta'\,e^{-f'\cdot\mathrm{CDF}} \tag{2a}$$

$$\mathrm{CDF} = \left[\exp\left(\alpha' - \frac{E'}{RT} + \beta' C\right)\right]\cdot C\cdot t \tag{2b}$$

where C is the *p*-TsOH molar concentrations (mol/L), R = 8.314 J/mol/K is the universal gas content, t is reaction time in min, T is reaction temperature in kelvins. E and E' are activation energy (J/mol). α, α' and β, β' are fitting parameters. θ and θ' are the fractions of slow reacting xylan and lignin, respectively. f and f' are the ratios of reaction rates between slow and fast xylan, and slow and fast lignin, respectively. The above equations will be used to fit to the xylan and lignin component dissolution data from mass balance analyses to obtain these parameters. The purpose of this type analyses are to use reaction severity CHF or CDF as a process scale-up factor, so process scale-up is not dependent on individual reaction condition. In other words, desired delignification can be achieved in scale-up runs as long as the same CDF is achieved by using a combination of *p*-TsOH concentration, temperature, and time to alleviate potential process constrains by individual reaction conditions on the scale-up facility.

Acetylation of Lignin. First, 0.1 g of lignin was dissolved in 2 mL of pyridine and acetic anhydride solution (1:1, v/v) and kept in a dark cabinet at room temperature for 72 h; then, the solution was added dropwise with constant stirring into 120 mL of ice-cold water containing 1 mL of HCl. The precipitated lignin acetate was separated by centrifugation and washed twice with DI water, discarding all supernatants, and then air-dried at room temperature for 48 h and then in a vacuum oven at 50 °C for an additional 24 h.

Nuclear Magnetic Resonance (NMR) Spectroscopic Analyses. NMR samples were prepared by dissolving 60 mg of lignin in 0.6 mL solution of dimethyl sulfoxide-d_6/pyridine-d_5 (4:1).[38] Spectra were recorded using a Bruker (Billerica, MA) 500 MHz AVANCE IIII NMR spectrometer equipped with a Prodigy (N_2-cooled) 5 mm gradient TCI (inverse configuration) $^1H/^{13}C/^{15}N$ cryo-probe. 2D ^{13}C-^1H spectra were referenced to the central dimethylsulfoxide solvent peak at δ_C 39.5 ppm and δ_H 2.5 ppm. Two-dimensional heteronuclear single-quantum coherence (HSQC) spectra were recorded at 25 °C using the standard hsqcetgpsisp 2.2 pulse program with the following parameters: acquisition time (AQ) of 85 ms using spectral width of 12 ppm in $F_2(^1H)$ dimension with 1024 data points (TD1) and 215 ppm in $F1(^{13}C)$ with 512 nonuniformly sampled data points (TD2); the number of scans (NS) was 40 with a 1 s interscan delay for a total acquisition time (expt) of 3 h. The $^1J_{C-H}$ used as 145 Hz. Prior to Fourier transformation, the data matrices were zero-filled up to 1024 points in the ^{13}C dimension and processed using typical matched Gaussian apodization (LB = −0.10, GB = 0.01) in F_2 and cosine-squared (SSB = 2) in F_1. Bruker Topspin 3.5pl7 was used for interactive integration of contours. We colored the spectral images using Adobe Illustrator CS6 and created the chemical structures using ChemDraw Pro 8.0.

2D ^{13}C-^1H HSQC NMR can determine specific carbon functionalities that cannot be identified using either ^{13}C or ^1H one-dimensional spectra.[39−41] Although such determinations by 2D HSQC are not inherently quantitative, the results can provide information about relative quantities of various functionalities based on per 100 Ar units. As illustrated, the total aromatic areas are defined as: $I(C9) = 0.5 \times I(S_{2,6}) + 0.5I(S'_{2,6}) + I(G2) + I(G'2) + I(S_{condensed})$. The content of internal linkages are calculated as: β-O-4 = $100 \times [I(\beta\text{-O-}4)]/[I(C9)]$; β-β = $100\times[I(\beta\text{-}\beta)]/[I(C9)]$; β-5 = $100 \times [I(\beta\text{-}5)]/[I(C9)]$. The content of $PB_{2,6}$ unit is also calculated based on per 100 Ar: PB = $100 \times 0.5 \times I[(PB_{2,6})]/[I(C9)]$. Content of aromatic units are relative (%): S = $100 \times 0.5 \times [I(S_{2,6})]/[I(C9)]$; S′ = $100 \times 0.5 \times [I(S'_{2,6})]/[I(C9)]$; G = $100 \times [I(G2)]/[I(C9)]$; G′ = $100 \times [I(G'2)]/[I(C9)] \times 100$. The S/G ratio is defined as: S/G = $[(S + S' + S_{condensed})]/[(G + G')]$.

Gel Permeation Chromatographic Analyses. The number and weight-averaged molecular weights, M_n and M_w, respectively, of the acetylated lignin samples were determined

DOI: 10.1021/acs.iecr.9b00931
Ind. Eng. Chem. Res. 2019, 58, 7063−7073

using an ion chromatographic system (ICS-3000, Dionex, Sunnyvale, CA) equipped with three 300 mm × 7.8 mm i.d. Phenogel 5U columns (10 000, 500, and 50 Å) and a guard column (Phenomenex, Torrance, CA).[42] Briefly, lignin acetate (50 mg) was dissolved in 2 mL of HPLC-grade tetrahydrofuran (THF), and 0.50 mL of the solution was injected into the GPC columns. THF was used as eluent at a flow rate of 1 mL/min. The column temperature was 30 °C. Polystyrene was used as standard for calibration. Absorption signals of lignin and polystyrene were detected using a variable wavelength detector at 280 and 254 nm, respectively.

Differential Scanning Calorimetric (DSC) Analyses. The lignin glass transition temperature T_g was obtained through DSC analyses using a calorimetric system (TA-DSC-Q20, TA Instruments). Aliquot samples of 3−5 mg were run at a heating rate of 10 °C/min between 40 and 400 °C under nitrogen flow (50 mL/min). The T_g of the lignin samples were derived using TA Universal Analysis software equipped with the instrument.

RESULTS AND DISCUSSION

Effects of *p*-TsOH fractionation severity on AHL production. The chemical compositions of fractionated cellulosic water insoluble solids (WISs) and the spent liquors along with each component retained on WISs are listed in Table 1. Fitting the data in Table 1 using eqs 1 and 2 resulted in adjustable parameters α = 44.03, α' = 25.78 and β = 1.04, β'=1.11, apparent activation energy E = 150 600 and E' = 98 000 (J/mol), the fraction of slow reacting xylan and lignin of θ = 0.248 and θ' = 0.497, respectively, and the ratios of reaction rates between slow and fast xylan f = 0.010 and between slow and fast lignin f' = 0.026. Excellent fittings of the data were obtained as shown in Figure 1. The results clearly indicate the two-phase behavior in AHF of poplar wood using *p*-TsOH, primarily due to the heterogeneity of xylan and lignin in wood. Approximately 65% xylan and 40% lignin can be rapidly (≤30 min) dissolved using *p*-TsOH with relatively low severities, i.e., CHF < 2 or CDF < 1.5, to produce lignin with low degree of condensation as will be discussed later. The dissolved xylan is mainly in the form of xylose or xylooligomers (not analyzed) due to the low severities employed. Furfural was undetectable except under higher severities at elevated temperature and extended reaction time (P40T96t180) with furfural concentration of 0.46 g/L. Our early study indicated that the dissolved xylan can be dehydrated into furfural at high yield using the *p*-TsOH in the spent liquor without additional catalysts.[33,43]

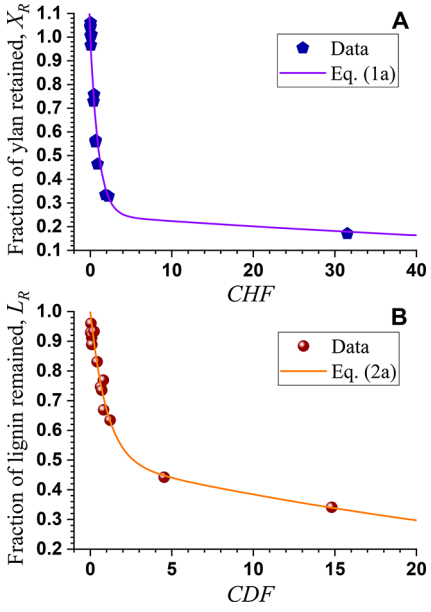

Figure 1. Predictions of xylan and lignin dissolution by *p*-TsOH fractionation of a poplar using a combined hydrolysis factor (CHF) and a combined delignification factor (CDF), respectively, in comparison with experimental data.

AHL Physical Properties. The physical appearance of precipitated and freeze-dried AHL, washed WIS, and spent liquor (Figure 2A−K) was compared to that of MWL and WIS from the MWL extraction process (Figure 2L). Overall, increasing fractionation severity through increasing *p*-TsOH concentration at the same fractionation temperature of 70 °C for the same duration of 30 min deepened the color of AHL, WIS, and spent liquor (Figures 2A−D). Very mild *p*-TsOH fractionations (CDF ≤ 0.24 and AHL yield < 10%; Table 1) with minimal AHL condensation as will be discussed in later (Table 2), produced WISs (Figures 2A,B,E,F) with very light color, similar to the WIS from MWL extraction process. These light colored WISs are excellent for direct blending with commercial bleached papermaking fibers as will be presented in the section for evaluation of papermaking potential.

Both the WISs and AHLs from very mild conditions have a pinkish color, whereas MWL has a yellow color. Increasing fractionation severity CDF to 1.2 with low degree of AHL condensation (NMR analyses in Table 2), the color of AHLs, WISs, and spent liquors were pinkish brown (Figure 2C,G,I−K), with the brown color becoming more pronounced with increasing CDF. For example, elevated fractionation temperature (Figure 2J) and extended fractionation time (Figure 2K) resulted in WISs, AHLs, and spent liquors with pronounced brown color. Further increase in fractionation severity CDF with substantial AHL condensation (Table 2) produced AHLs with dark brown and black colors, while WISs remained pinkish brown (Figure 2D,H).

Insight into the interplay of dissolution, depolymerization, and repolymerization during fractionation can be garnered by examining changes in AHL molecular weight with respect to fractionation severity and glass transition temperature. The molecular weight distribution probability density profiles of all fractionation conditions showed bimodal behavior, as shown in Figure 3A,B. We divided all of the AHLs into three groups based on the variations in M_w with respect to reaction severity CDF as listed in Table 3 and shown in Figure 3C: low severity group 1, CDF < 0.75; moderate severity group 2, 0.75 ≥ CDF < 2.0); severe severity group 3, CDF ≥ 2.0. At a low fractionation severity such as P25T70t30 (Figure 3A), with M_w = 5148 Da and T_g = 150 °C, only a comparatively small amount of lignin was dissolved (Table 1). Lignin dissolution should be dominated by physical aggregation in the hydrotropic system, after only mild depolymerization from the acid catalyst.[27−29] Depolymerization increased continuously with increasing severity as can be clearly seen from the depressing of the high molecular weight peak and the increasing in the low molecular weight peak in the distribution curves for group 1 in Figure 3A. M_w decreased continuously from approximately 5000 to 3500 Da as a result, and T_g was increased slightly from 150 to 157 °C as shown in Figure 3C. Within the boundary conditions of severity CDF < 0.75 and T_g = 150−157 °C

DOI: 10.1021/acs.iecr.9b00931
Ind. Eng. Chem. Res. 2019, 58, 7063−7073

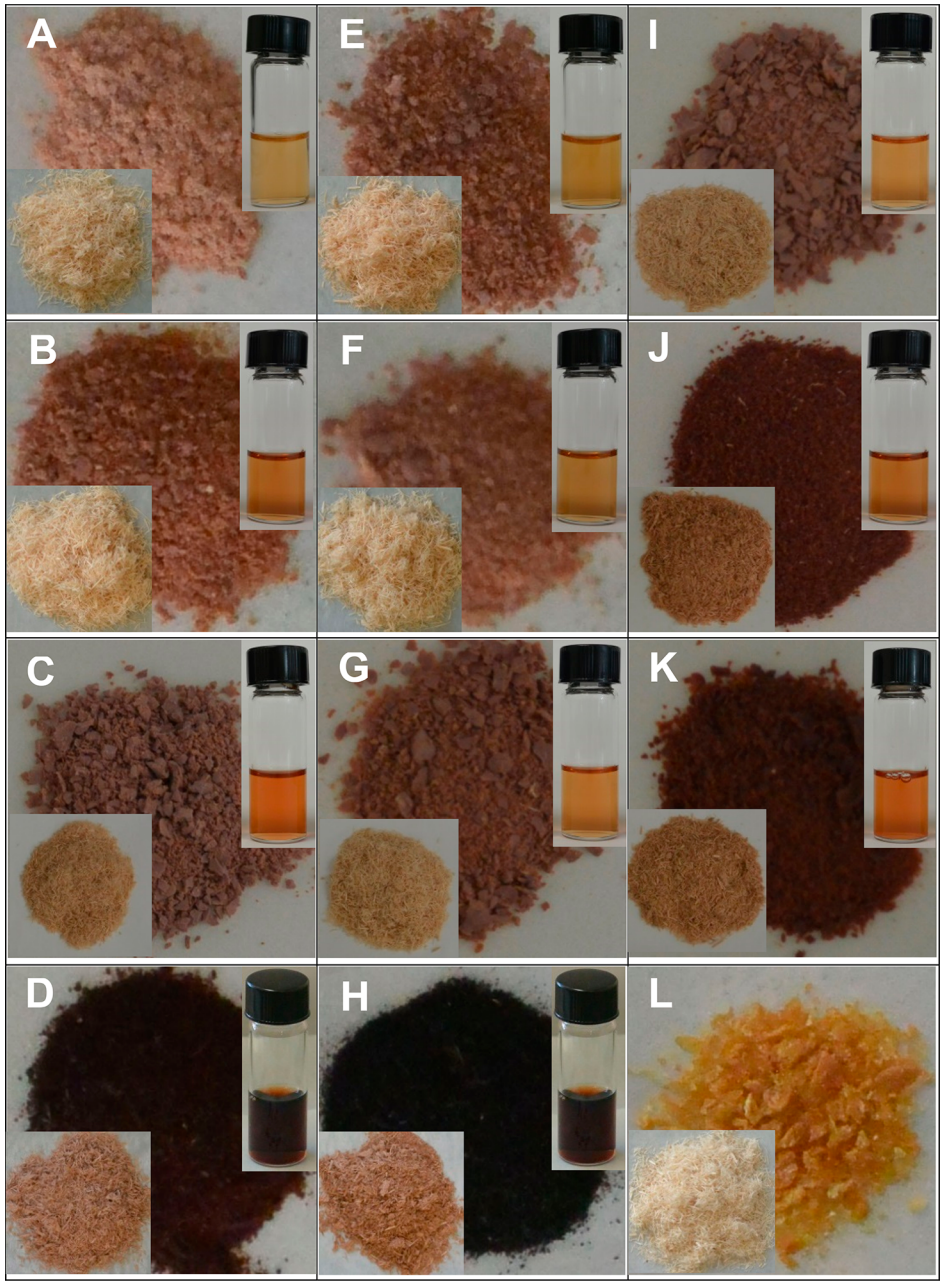

Figure 2. Photos of *p*-TsOH fractionated poplar AHL, washed WIS (left bottom corners), and spent liquor (bottles) along with MWL and cellulosic solids from MWL extraction. P25T70t30 (A); P40T70t30 (B); P55T70t30 (C); P67T70t30 (D); P25T70t60 (E); P40T60t30 (F); P50T70t30 (G); P40T95t180 (H); P40T80t30 (I); P30T95t30 (J); P30T80t115 (K); MWL (L).

(group 1), we can deduce some relative effects of the variable parameters. For example, comparing P30T80t60 (T_g = 157 °C and M_w = 3513) with P40T80t30 (T_g = 152 °C and M_w = 3743) we observe lower molecular weight and lower T_g with using 10% more acid for only half the time at a given temperature; comparing P40T50t30, P40T60t30, and P40T70t30 we observed minor temperature effects in the range of 50−70 °C.

Further increasing severity to CDF ≤ 2.0 shows a shift back toward higher molecular weights as shown by group 2 in Figure 3B where the low molecular weight peak was decreased and the high molecular weight peak was increased. As a result, M_w was increased from approximately 3500 to 4000 Da with T_g = 159 − 164 °C (Figure 3C). The molecular weight distribution curves shifted right. This may inform of conditions which transition from primarily depolymerization to lignin condensation. Condensation became substantial under the most severe conditions such as for group 3 in Figure 3B,C (CDF ≥ 2), which increased M_w to approximately 5000 and significantly increased T_g = 182 − 216 °C (Table 3, Figure 3C). The fact that T_g increased continuously with CDF but slowly under CDF < 2.0 suggests lignin condensation was always present but low and became significant only when CDF ≥ 2.0 and T_g increased rapidly.

AHL Chemical Structures from ^{13}C-^{1}H 2D NMR. 2D heterogeneous single quantum coherence (HSQC) NMR was used to estimate the main linkages in the AHLs. The spectra and main lignin substructures and linkages were assigned according to literature[39,40] and are depicted in Figure 4. As graphically summarized in Figure 5, mild batch *p*-TsOH

DOI: 10.1021/acs.iecr.9b00931
Ind. Eng. Chem. Res. 2019, 58, 7063−7073

Table 2. 2D ^{13}C-^{1}H NMR HSQC Spectral Analyses of Side Chains and Aromatic Units Present in AHLs from Batch *p*-TsOH Fractionations of Poplar

run labels[a]	CDF	$S_{2/6}$	$S'_{2/6}$	$S_{condensed}$	S	G	S/G	*p*-hydroxybenzoate (PB)	*β*-O-4 (%)	*β*-5 (%)	*β*-*β* (%)	AHL yield (%)
poplar MWL	0	52	5.0	0	57	43	1.3	22	58	3.2	2.7	
Poplar: Acid Hydrotropic Lignin (AHL)												
P40T50t30	0.03	54	0.8	0	55	45	1.2	34	62	3.5	2.9	7.1
P25T70t30	0.04	55	0.9	0	56	44	1.3	33	60	3.1	3.6	4.0
P40T60t30	0.09	55	0.7	0	56	44	1.3	32	61	3.4	2.9	7.9
P25T70t60	0.09	56	0.9	0	57	43	1.3	27	62	3.3	3.3	8.8
P32T70t30	0.10	55	0.9	0	56	44	1.3	29	62	4.0	3.5	11.1
P40T70t30	0.24	56	0.8	0.9	56	43	1.3	29	61	3.8	2.9	6.7
P30T80t60	0.42	59	0.9	2.6	62	38	1.6	26	61	3.2	3.4	16.9
P40T80t30	0.63	57	0.8	2.1	60	40	1.5	30	61	3.3	3.0	25.4
P50T70t30	0.71	58	0.8	3.4	63	37	1.7	34	59	3.1	3.1	26.5
P30T80t115	0.81	67	1.3	5.9	74	26	2.9	25	54	1.8	3.5	23.1
P30T95t30	0.82	65	1.4	11.2	78	22	3.5	25	46	1.9	3.4	33.1
P55T70t30	1.2	60	1.1	7.6	69	31	2.2	31	53	2.9	3.2	36.6
P67T70t30	4.5	68	2.0	19.4	89	11	8.4	35	25	2.0	3.4	55.8
P40T95t180	14.8	57	5.3	35.8	98	2.2	45	22	4.4	2.2	1.1	65.9
Birch: Salt (Sodium Xylenesulfonate, SX) Hydrotropic Lignin (SHL)[32]												
SX36T170t120			2		78	19	4.2		15.0	3.3	3.2	~68.0
SX+H_2O_2+Formic acid			3		73	22	3.4		11.8	3.2	3.0	~68.0

[a]P*xx*T*yy*t*zz*: stands for *p*-TsOH concentration (wt %), temperature (°C), and total flow time (min)

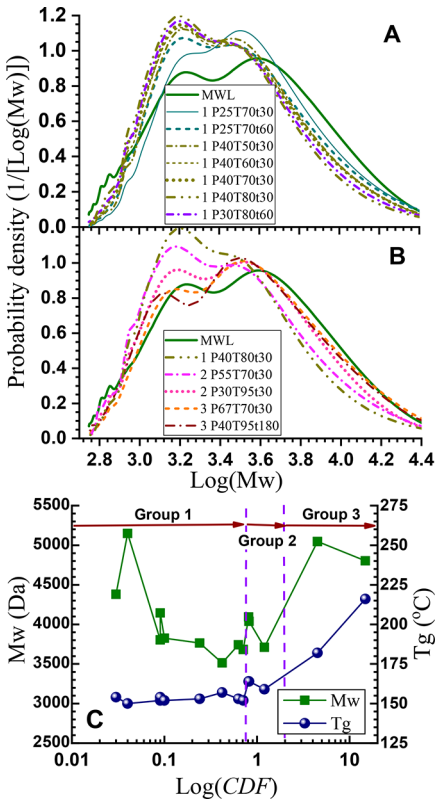

Figure 3. Comparisons of GPC measured AHL molecular distributions under different fractionation conditions. The first number in the legend is the AHL group number listed in Table 3. A: groups 1; B: groups 2–3; C: correlation of M_w and T_g with reaction severity CDF.

fractionations (i.e., CDF < 0.75, group 1), resulted in AHLs similar (Figure 4A,B,F) to MWL (Figure 4E), retaining nearly all of the *β*-O-4 linkages. Increasing fractionation severity up to CDF = 1.2 (group 2), except the run at extreme temperature P30T95t30, resulted in only slight reduction, less than 15% compared to MWL, of *β*-O-4 linkages (Figure 5), but with AHL yield of approximately 37% at CDF = 1.2 (Table 2). Further increasing fractionation severity improved AHL yield but also resulted in increased reduction in *β*-aryl ether linkages. For example, at CDF = 4.5 (P67T70t30, group 3) AHL yield was increased to 56% (Table 2), but *β*-aryl ether linkages (Figure 4C) were reduced to 25% (Table 2) or reduced by 56% compared to MWL. Further increase in severity, by using extended fractionation time and elevated temperature (P40T95t180 with CDF = 14.8), increased AHL yield to 66%; however, almost all *β*-aryl ether linkages were eliminated (Figure 4D), retaining only 4.4% (Table 2), or a 92% reduction.

Under severe conditions, acid-catalyzed formation of a benzylic cationic intermediate can undergo loss of a proton and hydrolysis to yield Hibbert's ketone (HK), identified in the 2D NMR spectra (Figure 4C,D,G,H; δ_C/δ_H = 67.1/4.19 ppm, *γ*-position; δ_C/δ_H = 44.5/3.67 ppm (*α*-position),[42] or this intermediate can go through a retro-Prins reaction followed by hydrolysis to give homobenzaldehydes and formaldehyde.[21] The generated aldehydes can potentially undergo condensation reactions leading to extensive C–C bond formation. In addition, trapping of the benzylic cations by the electron rich aromatic groups in lignin can lead to further C–C bond formation. As Figure 4 shows, the HK from cleavage of the *β*-ether units was not observed or barely visible in the HSQC NMR spectra of the AHLs from mild conditions, with a very weak HK_γ signal appearing under P50T70t30 with CDF = 0.71, but no visible HK_α signal (Figure 4B). The HK contour area increased only slightly with increasing CDF under severe conditions (Figure 4C,D,G,H).

Interestingly, we note that temperature and time played a more critical role than acid concentration. For example, AHL from the two runs with moderate temperatures and fraction time: P40T80t30 (CDF = 0.63) and P50T70t30 (CDF = 0.71) have essentially unchanged *β*-O-4 linkages compared to MWL,

DOI: 10.1021/acs.iecr.9b00931
Ind. Eng. Chem. Res. 2019, 58, 7063–7073

Table 3. Mean Molecular Weights and Glass Transition Temperatures of AHL Samples Obtained under Various Hydrotropic Fractionation Conditions

lignin sample[a]	group	CDF	M_n (Da)	M_w (Da)	PDI	T_g (°C)
poplar MWL	0	0	1726	4115	2.4	137
Poplar: Acid Hydrotropic Lignin (AHL)						
P40T50t30	1	0.03	1984	4380	2.2	154
P25T70t30	1	0.04	2216	5148	2.3	150
P40T60t30	1	0.09	1900	3803	2.0	152
P25T70t60	1	0.09	1982	4145	2.1	154
P32T70t30	1	0.10	1932	3827	2.0	152
P40T70t30	1	0.24	1741	3765	2.2	153
P30T80t60	1	0.42	1847	3513	1.9	157
P40T80t30	1	0.63	1740	3743	2.2	153
P50T70t30	1	0.71	1706	3682	2.2	152
P30T80t115	**2**	**0.81**	**1981**	**4094**	**2.1**	**164**
P30T95t30	**2**	**0.82**	**1857**	**4038**	**2.2**	**164**
P55T70t30	**2**	**1.2**	**1730**	**3710**	**2.2**	**159**
P67T70t30	3	4.5	1949	5046	2.6	182
P40T95t180	3	14.8	1817	4803	2.6	216
Birch: Salt (Sodium Xylenesulfonate, SXS) Hydrotrope Lignin (SHL)[32]						
SXS36T170t120			1035	5305	5.1	
SXS+H_2O_2+formic acid			1143	5910	5.2	

[a]P*xx*T*yy*t*zz*: stands for *p*-TsOH concentration (wt %), temperature (°C), and total flow time (min)

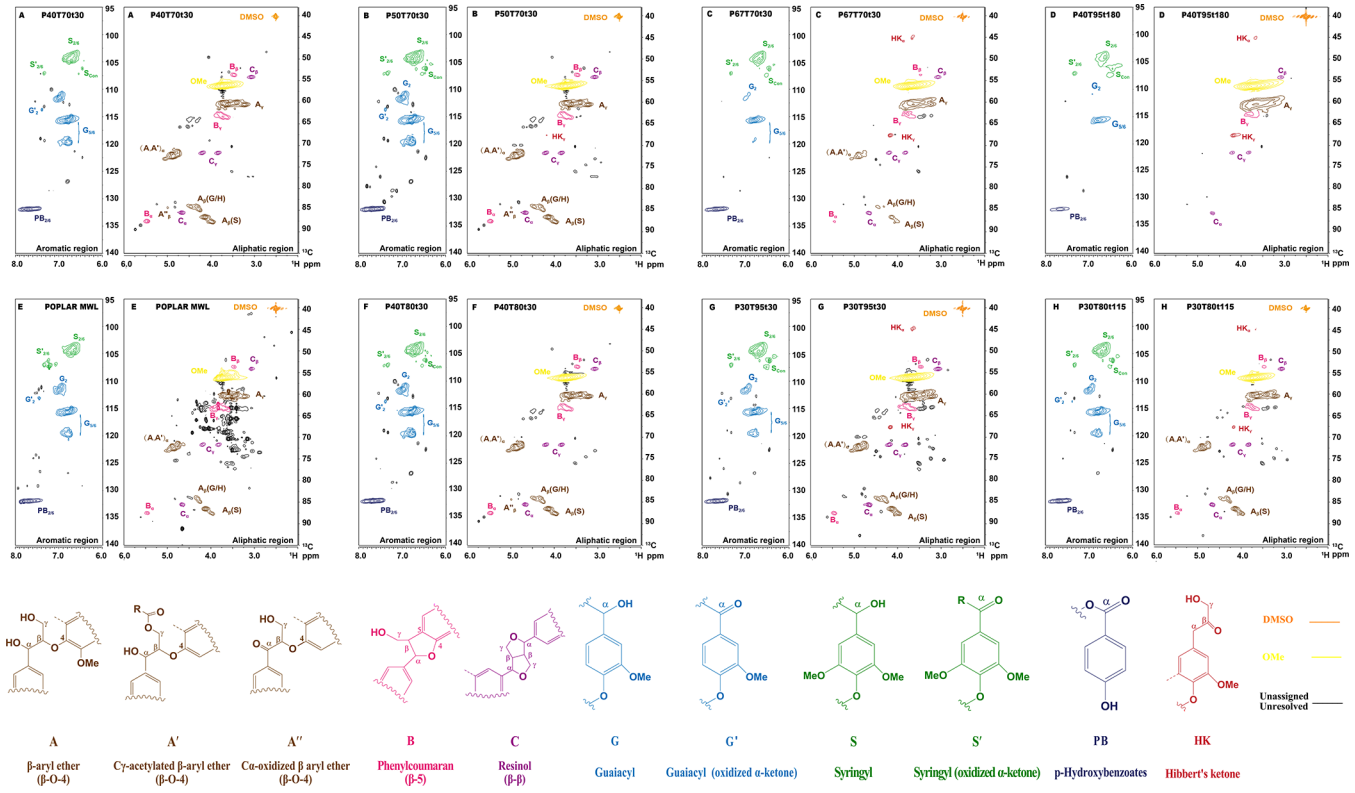

Figure 4. 2D ^{13}C-^{1}H NMR HSQC spectra of selected AHL samples shown in Figure 2 in comparison with the spectra of MWL. P40T70t30 (A); P554T70t30 (B); P67T70t30 (C); P40T95t180 (D); MWL (E); P40T80t30 (F); P30T95t30 (G); P30T80t115 (H).

whereas P30T95t30 (CDF = 0.82), at a lower *p*-TsOH concentration of 30 wt % for the same duration of 30 min but with elevated temperature of 95 °C, has a much lower *β*-O-4 linkage content of 46% (Table 2, Figure 5), or approximately 25% reduction. Also, examining AHLs from very similar severities of CDF = 0.81 and 0.82 with the same acid content of 30% (P30T80t115 and P30T95t30) shows approximately 12 and 25% reduction of *β*-O-4 linkage and a doubling and more than tripling of syringyl condensation (Table 2), respectively, compared with AHL from CDF = 0.71 (P50T70t30). This indicates that elevated temperature and extended fractionation duration play a critical role in eliminating *β*-O-4 linkages to form condensed lignin and is clearly reflected in Figure 5 as the data from P30T95t30 (CDF = 0.81) and P30T80t115 (CDF = 0.82) do not lie on the general data trend line.

DOI: 10.1021/acs.iecr.9b00931
Ind. Eng. Chem. Res. 2019, 58, 7063−7073

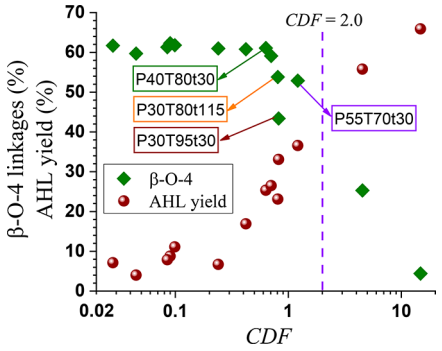

Figure 5. Effects of *p*-TsOH batch fractionation severity expressed by the combined delignification factor (CDF) on the yield and *β*-O-4 linkage content of the resultant AHL.

Because AHL yield is a critical consideration, it was also plotted in Figure 5. AHL yield of 50% corresponding to a CDF ≈ 3, approximately half of the *β*-O-4 linkages are retained. The ratio of S to G is also significantly altered at CDF ≈ 3, as inferred from extrapolation of values in Table 2. At severities CDF < 1, the S/G ratio and *β*-O-4 changed little (except for those two runs with higher temperature or extended fractionation time), suggesting that the AHL structure was not very significantly altered from that of MWL, however the AHL yield was < 26%. At CDF = 1.2, the AHF yield improved to ∼ 37% with a ∼ 10% reduction in *β*-O-4.

Comparison of AHL with Lignin from Salt-Based Hydrotropic Fractionation. Despite salt-based hydrotropic fractionation being well-studied for wood pulping and salt hydrotropic fractionation being used as a pretreatment method to produce sugar enzymatically from lignocelluloses,[31,32] limited studies were devoted to characterize salt-based hydrotropic lignin. Here we compared our AHL properties with those of salt hydrotropic birch wood lignin (the only work we found in the literature).[32] As listed in Table 2, sodium xylenesulfonate (at 36%) fractionation at 170 °C for 120 min (much higher temperature and longer time than those used in the present study) only achieved a lignin yield of approximately 68%. The resultant lignin had a *β*-O-4 linkage content of approximately 15%. When adding formic acid and peroxide, the content of *β*-O-4 linkages was reduced to 11.8%, indicating these two lignins were condensed. Contents of *β*-5 and *β*-*β* were similar to our AHLs. Because only one condition was reported in the literature work,[32] it is difficult to know whether a low fractionation severity (i.e., a low lignin yield), similar to what the present study reported in Table 2, would result in a lignin with less condensation (higher *β*-O-4 content), similar to our AHL (Table 2). It is expected, however, that a reduced temperature often results in substantially low delignification for salt-based hydrotropic fractionation. Furthermore, the results of commercial technical lignin obtained at elevated temperatures and prolonged reaction times all showed great degree of condensation.[9] The discussion in the previous section also suggests high temperature and extended fractionation resulting in lignin condensation.

Salt fractionation produced a lignin with a slightly greater weight averaged molecular weight M_w but a smaller number averaged M_n than those of our AHLs (Table 3). As we discussed in section "AHL Physical Properties", the greater M_w is most likely due to lignin condensation, while a much smaller M_n indicates substantially more lignin depolymerization than AHLs. As a result, salt-based hydrotropic lignin had a much greater polydispersity than AHLs (Table 3). It is expected that T_g (not reported in literature) will be higher than those AHLs reported in Table 3 due to lignin condensation.

***p*-TsOH Fractionated Cellulosic Solids as Papermaking Fibers.** Producing papermaking fibers is a higher-value use of cellulosic materials than producing sugars. To demonstrate the utility of AH fractionated cellulosic solids, we used the washed WIS from P40T70t30 (bottom left corner in Figure 2B) to substitute bleached eucalyptus pulp (BEP) fibers in papermaking. The extent of substitution was varied from 0 (control) to 40%. The WIS has a solid yield 94.6% from P40T70t30 (Table 1), so it is very similar to commercial thermal mechanical pulp. The WIS was refined using a laboratory stone disk mill at 2% solids loading (Super-MassColloider, MKZA 6−2, Disk model: MDGA 6−80#, Masuko Sangyo Co., Ltd., Japan) for one pass. The energy consumption was 2.5 MJ/kg. The final pulp Canadian standard freeness (CSF) was 448 mL. The BEP was also refined using a Valley Beater (Test Machines, Inc.) to CSF of 562 mL. Handsheets were made according to TAPPI standard method T220. Handsheet tensile strength and opacity were measured according to standard TAPPI Test Method T494 and T519, respectively. As shown in Figure 6, specific tensile strength of

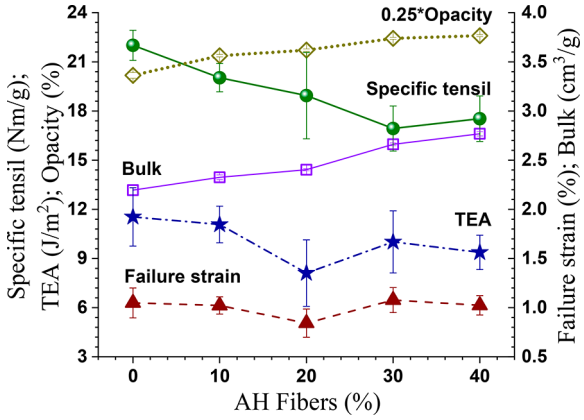

Figure 6. Effects of the degree of AH fiber substitution for bleached eucalyptus pulp fibers on handsheet mechanical and optical properties.

handsheets was reduced by approximately 20% at 40% substitution of BEP fibers with AH fibers. This reduction is due to the fact AH fibers are very similar to mechanical pulp fibers with very high lignin content and therefore resulted in reduced hydrogen bonding. Cellulose degradation by *p*-TsOH had limited contribution to this reduction. Handsheet strain was not reduced. It is noteworthy that handsheet bulk was increased by 26% at 40% substitution. The increased bulk resulted in an increase in handsheet opacity by 12%. In papermaking, paper strength is only one measure of paper properties. Increasing paper bulk or reducing density can reduce fiber consumption while increasing opacity. It should be pointed out that bleaching AH is often needed in practice for blending with chemical pulps. However, AH fibers with low degree of condensation are easier to bleach using common paper mill bleaching chemicals based on our unpublished lab study. We expect that the bleached AH fibers will retained much of their stiffness for high bulk papers and can be excellent material for papermaking applications.

DOI: 10.1021/acs.iecr.9b00931
Ind. Eng. Chem. Res. 2019, 58, 7063−7073

Evaluation of *p*-TsOH Recyclability. Preliminary experiments were carried out to demonstrate *p*-TsOH recovery efficiency. As a first step in evaluating the recovery of *p*-TsOH, we compared the amount of fresh *p*-TsOH applied in each fractionation with the amount collected from the spent liquor and filtrates from multiple-step washing of the fractionated cellulosic solids. The amounts of *p*-TsOH in the fresh solution, the spent liquor, and the filtrates were all measured by HPLC. A total of four sets of experiments were carried out under two different fractionation conditions using two different poplar samples of the same source but different grinding. Aliquots of 10 g of poplar (oven dry) was applied in these experiments using 100 g of *p*-TsOH aqueous solution with two different loadings of *p*-TsOH at nominal amounts of 40 and 67 g, respectively. Each washing step used 100 g of water. Promisingly, the *p*-TsOH loss was less than 1.5% for all four runs (Table 4).

Table 4. Comparisons of the Amount of *p*-TsOH Applied in the Fresh *p*-TsOH Liquors with the Amount Collected from the Spent Liquor and Filtrates of Multiple-Step Washing of Fractionated Solids[a]

run	P40T95t178	P67T70t26	P40T95t178H	P67T70t26H
nominal amounts (g)	40	67	40	67
	Amounts Measured by HPLC			
fresh liquor (g)	43	72	43	70
spent liquor (g)	39	64	37	64
filtrate – first wash (g)	3.1	6.9	4.7	4.5
filtrate – second wash (g)	0.6	0.3	0.4	0.5
filtrate – third wash (g)	0.004	ND	0.001	ND
filtrate – fourth wash (g)	ND	ND	ND	ND
total collected (g)	42	72	42	69
p-TsOH loss (%)	1.2	0.9	1.3	1.0

[a]ND stands for not detectable.

We also conducted preliminary evaporation of the diluted spent liquor of 2 wt % under atmospheric condition and found that less than 5% of *p*-TsOH went to the condensate after being concentrated to approximately 20 wt %. The amount of *p*-TsOH in the condensate can be reduced through optimization in industrial evaporators and can also be reclaimed through adsorption using hyper-cross-linked porous polymers as recently demonstrated[44] or simply through evaporation. These preliminary results demonstrate potential for a high rate of *p*-TsOH recovery, of approximately 95% with only two washing steps, after 2 to 3 cycles of reuse and recovery, and will be the subject of future study.

Previously, we evaluated the reactivity of *p*-TsOH spent liquor without lignin separation.[29] The chemical composition of the fractionated solids from the first and second cycle were compared under two conditions, at P55T80t20 and P80T80t20. In the second cycle, the spent liquor was refreshed by adding 10% fresh *p*-TsOH solution so as to compensate for spent liquor loss in the fractionated solids. The differences in the compositions of WISs from the first and second cycle were negligible, indicating that reusing a substantial amount of spent liquor (approximately 90%) is feasible without reducing fractionation efficiency. This can substantially reduce the load of the recovery cycle.

CONCLUSIONS

This study demonstrated a potentially viable pathway for complete lignocellulose valorization through acid hydrotropic fractionation (AHF) using a relatively inexpensive commercial aromatic acid catalyst, *p*-toluenesulfonic acid (*p*-TsOH). Poplar wood was rapidly and selectively fractionated in 30 min at temperatures below the boiling point of water resulting in a cellulose-rich solid fraction that was valorized as papermaking fibers. The dissolved hemicelluloses can be dehydrated into furfural using the *p*-TsOH in the spent liquor without additional catalysts. The acid hydrotrope dissolved lignin (AHL) was isolated and characterized. At low fractionation severities and the expense of high yield, AHLs have well-preserved β-aryl ether bonds with large molecular weight and low glass transition temperature, similar to mill wood lignin (MWL), excellent for direct application in composites or for producing lignin aromatics through subsequent depolymerization. However, at a small reduction in aryl-ether linkages of approximately 15%, moderate AHL yield of 40% can be obtained, which is not achievable by most existing fractionation processes. Moderate reaction temperature and short reaction time (i.e., $\leq$80 °C for $\leq$30 min) is the key to produce AHL with minimal condensation.

AUTHOR INFORMATION

Corresponding Author

*E-mail: junyong.zhu@usda.gov. Tel. +1-608 231 9520.

ORCID

Jinlan Cheng: 0000-0001-8462-6606

J. Y. Zhu: 0000-0002-5136-0845

Notes

The authors declare the following competing financial interest(s): Zhu is a co-inventor of the p-TsOH fractionation process.

ACKNOWLEDGMENTS

This work was partially supported by U.S. Forest Service (USFS), Jiangsu Provincial Key Laboratory of Pulp and Paper Science and Technology under grant No. 201523 and Chinese Scholarship Council. These supports made the visiting appointments of J.C., Q.M., and J.Z. at the USFS Forest Products Laboratory (FPL) possible. We also would like to acknowledge Roland Gleisner (FPL) for hammer milling the poplar wood, Fred Matt (FPL) for conducting chemical composition analyses, Doreen Mann (FPL) for Soxhlet extraction and DSC analyses, Sally Ralph (FPL) and Richard Reiner (FPL) for assistance in producing MWL, and Dr. Xuejun Pan and Ning Li of University of Wisconsin-Madison for allowing us using his lab equipment, assistance in GPC analyses, and helpful discussion.

REFERENCES

(1) Zalesny Jr, R. S.; Donner, D. M.; Coyle, D. R.; Headlee, W. L. An approach for siting poplar energy production systems to increase productivity and associated ecosystem services. *For. Ecol. Manage.* **2012**, *284*, 45–58.

DOI: 10.1021/acs.iecr.9b00931
Ind. Eng. Chem. Res. 2019, 58, 7063–7073

(2) Zalesny, R. S. J.; Cunningham, M. W.; Hall, R. B.; Mirck, J.; Rockwood, D. L.; Stanturf, J. A.; Volk, T. A. Woody biomass from short rotation energy crops In *Sustainable Production of Fuels, Chemicals, and Fibers from Forest Biomass*; Zhu, J. Y., Zhang, X., Pan, X. J., Eds.; American Chemical Society: Washington, DC, 2011; pp 27−63
(3) Pan, X.; Gilkes, N.; Kadla, J.; Pye, K.; Saka, S.; Gregg, D.; Ehara, K.; Xie, D.; Lam, D.; Saddler, J. Bioconversion of hybrid poplar to ethanol and co-products using an organosolv fractionation process: Optimization of process yields. *Biotechnol. Bioeng.* **2006**, *94* (5), 851−861.
(4) Zhu, J. Y.; Pan, X. J.; Wang, G. S.; Gleisner, R. Sulfite pretreatment (SPORL) for robust enzymatic saccharification of spruce and red pine. *Bioresour. Technol.* **2009**, *100* (8), 2411−2418.
(5) Ewanick, S. M.; Bura, R.; Saddler, J. N. Acid-catalyzed steam pretreatment of lodgepole pine and subsequent enzymatic hydrolysis and fermentation to ethanol. *Biotechnol. Bioeng.* **2007**, *98* (1), 737−746.
(6) Iakovlev, M.; van-Heiningen, A. Efficient fractionation of spruce by SO2-ethanol-water treatment: Closed mass balances for carbohydrates and sulfur. *ChemSusChem* **2012**, *5* (8), 1625−1637.
(7) Brandt, A.; Ray, M. J.; To, T. Q.; Leak, D. J.; Murphy, R. J.; Welton, T. Ionic liquid pretreatment of lignocellulosic biomass with ionic liquid-water mixtures. *Green Chem.* **2011**, *13* (9), 2489−2499.
(8) Shuai, L.; Amiri, M. T.; Questell-Santiago, Y. M.; Héroguel, F.; Li, Y.; Kim, H.; Meilan, R.; Chapple, C.; Ralph, J.; Luterbacher, J. S. Formaldehyde stabilization facilitates lignin monomer production during biomass depolymerization. *Science* **2016**, *354* (6310), 329−333.
(9) Rinaldi, R.; Jastrzebski, R.; Clough, M. T.; Ralph, J.; Kennema, M.; Bruijnincx, P. C. A.; Weckhuysen, B. M. Paving the Way for Lignin Valorisation: Recent Advances in Bioengineering, Biorefining and Catalysis. *Angew. Chem., Int. Ed.* **2016**, *55* (29), 8164−8215.
(10) Kringstad, K. P.; Mörck, R. ^{13}CNMR Spectra of Kraft Lignins. *Holzforschung* **1983**, *37* (5), 237−244.
(11) Gellerstedt, G.; Lindfors, E. L. Structural changes in lignin during kraft pulping. *Holzforschung* **1984**, *38* (3), 151−158.
(12) Ragauskas, A. J.; Beckham, G. T.; Biddy, M. J.; Chandra, R.; Chen, F.; Davis, M. F.; Davison, B. H.; Dixon, R. A.; Gilna, P.; Keller, M. Lignin valorization: Improving lignin processing in the biorefinery. *Science* **2014**, *344* (6185), 1246843.
(13) Davis, R. T.; Scarlata, L.; Tan, C.; Ross, E.C.D.; Lukas, J.; Sexton, J. D. *Process design and economics for the conversion of lignocellulosic biomass to hydrocarbons: Dilute-acid and enzymatic deconstruction of biomass to sugars and catalytic conversion of sugars to hydrocarbons*; NREL/TP-5100−62498, Contract No. DE-AC36-08GO28308; National Renewable Energy Laboratory, 2015.
(14) Schutyser, W.; Renders, T.; Van Den Bosch, S.; Koelewijn, S. F.; Beckham, G. T.; Sels, B. F. Chemicals from lignin: An interplay of lignocellulose fractionation, depolymerisation, and upgrading. *Chem. Soc. Rev.* **2018**, *47* (3), 852−908.
(15) Renders, T.; Van Den Bosch, S.; Koelewijn, S. F.; Schutyser, W.; Sels, B. F. Lignin-first biomass fractionation: The advent of active stabilisation strategies. *Energy Environ. Sci.* **2017**, *10* (7), 1551−1557.
(16) Galkin, M. V.; Samec, J. S. M. Lignin Valorization through Catalytic Lignocellulose Fractionation: A Fundamental Platform for the Future Biorefinery. *ChemSusChem* **2016**, *9* (13), 1544−1558.
(17) Van Den Bosch, S.; Schutyser, W.; Vanholme, R.; Driessen, T.; Koelewijn, S. F.; Renders, T.; De Meester, B.; Huijgen, W. J. J.; Dehaen, W.; Courtin, C. M.; Lagrain, B.; Boerjan, W.; Sels, B. F. Reductive lignocellulose fractionation into soluble lignin-derived phenolic monomers and dimers and processable carbohydrate pulps. *Energy Environ. Sci.* **2015**, *8* (6), 1748−1763.
(18) Sun, Z.; Bottari, G.; Afanasenko, A.; Stuart, M. C. A.; Deuss, P. J.; Fridrich, B.; Barta, K. Complete lignocellulose conversion with integrated catalyst recycling yielding valuable aromatics and fuels. *Nature Catalysis.* **2018**, *1* (1), 82−92.
(19) Wang, S.; Shuai, L.; Saha, B.; Vlachos, D. G.; Epps, T. H. From Tree to Tape: Direct Synthesis of Pressure Sensitive Adhesives from Depolymerized Raw Lignocellulosic Biomass. *ACS Cent. Sci.* **2018**, *4* (6), 701−708.
(20) Sun, Z.; Fridrich, B.; De Santi, A.; Elangovan, S.; Barta, K. Bright Side of Lignin Depolymerization: Toward New Platform Chemicals. *Chem. Rev.* **2018**, *118* (2), 614−678.
(21) Lancefield, C. S.; Panovic, I.; Deuss, P. J.; Barta, K.; Westwood, N. J. Pre-treatment of lignocellulosic feedstocks using biorenewable alcohols: Towards complete biomass valorisation. *Green Chem.* **2017**, *19* (1), 202−214.
(22) Si, X.; Lu, F.; Chen, J.; Lu, R.; Huang, Q.; Jiang, H.; Taarning, E.; Xu, J. A strategy for generating high-quality cellulose and lignin simultaneously from woody biomass. *Green Chem.* **2017**, *19* (20), 4849−4857.
(23) Rahimi, A.; Ulbrich, A.; Coon, J. J.; Stahl, S. S. Formic-acid-induced depolymerization of oxidized lignin to aromatics. *Nature* **2014**, *515* (7526), 249−252.
(24) Luterbacher, J. S.; Azarpira, A.; Motagamwala, A. H.; Lu, F.; Ralph, J.; Dumesic, J. A. Lignin monomer production integrated into the y-valerolactone sugar platform. *Energy Environ. Sci.* **2015**, *8* (9), 2657−2663.
(25) Glasser, W. G.; Loos, R.; Cox, B.; Cao, N. Melt-blown compostable polyester films with lignin. *Tappi J.* **2017**, *16* (3), 111−121.
(26) Barana, D.; Ali, S. D.; Salanti, A.; Orlandi, M.; Castellani, L.; Hanel, T.; Zoia, L. Influence of Lignin Features on Thermal Stability and Mechanical Properties of Natural Rubber Compounds. *ACS Sustainable Chem. Eng.* **2016**, *4* (10), 5258−5267.
(27) Eastoe, J.; Hatzopoulos, M. H.; Dowding, P. J. Action of hydrotropes and alkyl-hydrotropes. *Soft Matter* **2011**, *7* (13), 5917−5925.
(28) Das, S.; Paul, S. Mechanism of hydrotropic action of hydrotrope sodium cumene sulfonate on the solubility of di-t-butylmethane: A molecular dynamics simulation study. *J. Phys. Chem. B* **2016**, *120* (1), 173−183.
(29) Chen, L.; Dou, J.; Ma, Q.; Li, N.; Wu, R.; Bian, H.; Yelle, D. J.; Vuorinen, T.; Fu, S.; Pan, X.; Zhu, J. Y. Rapid and near-complete dissolution of wood lignin at ≤80 °C by a recyclable acid hydrotrope. *Sci. Adv.* **2017**, *3* (9), No. e1701735.
(30) Procter, A. R. A review of hydrotropic pulping. *Pulp Pap. Mag. Can.* **1971**, *72* (8), 67−74.
(31) Mou, H.; Li, B.; Fardim, P. Pretreatment of corn stover with the modified hydrotropic method to enhance enzymatic hydrolysis. *Energy Fuels* **2014**, *28* (7), 4288−4293.
(32) Gabov, K.; Gosselink, R. J. A.; Smeds, A. I.; Fardim, P. Characterization of lignin extracted from birch wood by a modified hydrotropic process. *J. Agric. Food Chem.* **2014**, *62* (44), 10759−10767.
(33) Ma, Q.; Zhu, J.; Gleisner, R.; Yang, R.; Zhu, J. Y. Valorization of wheat straw using a recyclable hydrotrope at low temperatures (≤90 °C). *ACS Sustainable Chem. Eng.* **2018**, *6*, 14480−14489.
(34) Luo, X.; Gleisner, R.; Tian, S.; Negron, J.; Zhu, W.; Horn, E.; Pan, X. J.; Zhu, J. Y. Evaluation of mountain beetle infested lodgepole pine for cellulosic ethanol production by SPORL pretreatment. *Ind. Eng. Chem. Res.* **2010**, *49* (17), 8258−8266.
(35) Zhu, W.; Houtman, C. J.; Zhu, J. Y.; Gleisner, R.; Chen, K. F. Quantitative predictions of bioconversion of aspen by dilute acid and SPORL pretreatments using a unified combined hydrolysis factor (CHF). *Process Biochem.* **2012**, *47*, 785−791.
(36) Zhao, X.; Zhou, Y.; Liu, D. Kinetic model for glycan hydrolysis and formation of monosaccharides during dilute acid hydrolysis of sugarcane bagasse. *Bioresour. Technol.* **2012**, *105*, 160−168.
(37) Harris, J. F.; Baker, A. J.; Connor, A. H.; Jeffries, T. W.; Minor, J. L.; Pettersen, R. C.; Scott, R. W.; Springer, E. L.; Wegner, T. H.; Zerbe, J. I. *Two-stage, dilute sulfuric acid hydrolysis of wood: an investigation of fundamentals*; General Technical Report, GTR-FPL-045; USDA Forest Service, Forest Products Laboratory: Madison, WI, 1985

DOI: 10.1021/acs.iecr.9b00931
Ind. Eng. Chem. Res. 2019, 58, 7063−7073

(38) Kim, H.; Ralph, J. Solution-state 2D NMR of ball-milled plant cell wall gels in DMSO-d6/pyridine-d5. *Org. Biomol. Chem.* **2010**, *8* (3), 576−591.
(39) Del Río, J. C.; Rencoret, J.; Prinsen, P.; Martínez, A. T.; Ralph, J.; Gutiérrez, A. Structural characterization of wheat straw lignin as revealed by analytical pyrolysis, 2D-NMR, and reductive cleavage methods. *J. Agric. Food Chem.* **2012**, *60* (23), 5922−5935.
(40) Yelle, D. J.; Ralph, J.; Frihart, C. R. Characterization of nonderivatized plant cell walls using high-resolution solution-state NMR spectroscopy. *Magn. Reson. Chem.* **2008**, *46* (6), 508−517.
(41) Liu, C.; Wang, X.; Lin, F.; Zhang, H.; Xiao, R. Structural elucidation of industrial bioethanol residual lignin from corn stalk: A potential source of vinyl phenolics. *Fuel Process. Technol.* **2018**, *169*, 50−57.
(42) Li, N.; Li, Y.; Yoo, C. G.; Yang, X.; Lin, X.; Ralph, J.; Pan, X. An uncondensed lignin depolymerized in the solid state and isolated from lignocellulosic biomass: A mechanistic study. *Green Chem.* **2018**, *20* (18), 4224−4235.
(43) Ji, H.; Chen, L.; Zhu, J. Y.; Gleisner, R.; Zhang, X. Reaction kinetics based optimization of furfural production from corncob using a fully recyclable solid acid. *Ind. Eng. Chem. Res.* **2016**, *55* (43), 11253−11259.
(44) Woodward, R. T.; Kessler, M.; Lima, S.; Rinaldi, R. Hypercrosslinked microporous polymer sorbents for the efficient recycling of a soluble acid catalyst in cellulose hydrolysis. *Green Chem.* **2018**, *20* (10), 2374−2381.

DOI: 10.1021/acs.iecr.9b00931
Ind. Eng. Chem. Res. 2019, 58, 7063−7073